J Turk Spinal Surg 2025;36(3):103-109
DOI: 10.4274/jtss.galenos.2025.39200

BILATERAL CROSSING LAMINAR SCREW FIXATION IN LUMBAR SPONDYLOLYSIS: CT-BASED ANATOMICAL PARAMETERS

Burhan Oral Güdü[1], Belgin Karan[2]

[1]*Sefaköy Medipol University Hospital, Department of Neurosurgery, İstanbul, Türkiye*
[2]*Sefaköy Medipol University Hospital, Department of Radiology, İstanbul, Türkiye*

ABSTRACT

Objective: To evaluate computed tomography (CT)-based linear and angular anatomical parameters critical for crossing laminar screws (CLS) fixation of pars interarticularis defects in spondylolysis (SPL).

Materials and Methods: Two readers independently analyzed 110 lumbar CT scans of patients with bilateral SPL using multiplanar reconstruction in Centricity software to determine the optimal CLS trajectories. The ideal CLS trajectory was defined as originating from the spinolaminar junction contralateral to the targeted pars defect, passing through the intralaminar region, pars defect, pars neck, and pedicle, and ending at the lateral or superior cortex of the pedicle, maximizing bone engagement. Linear and angular parameters required for CLS fixation were assessed along the defined screw trajectory.

Results: CLS trajectory length significantly decreased from L5 to L3 (52, 43, and 38 mm, respectively) (p>0.05). The laminar height increased significantly from L5 to L3 (7-11 mm). Laminar width was greatest at L5 (10 mm) and similar at L3 and L4 (7 mm). The spinolaminar height significantly increased from L5 to L3 (14-19 mm). Spinolaminar angle was highest at L3 (45°) and similar at L4 and L5 (40°). Coronal angle increased significantly from L5 to L3 (9°-23°). Excellent inter- and intra-reader reliabilities were observed for all measurements.

Conclusion: For the fixation of pars defects at the L3-L5 levels using CLS, a screw length of 4-5 cm and a diameter of 4.5 mm appear to be appropriate. Laminar width and height, along with the spinolaminar angle and height, are fundamental anatomical factors for ensuring safe CLS placement.

Keywords: Spondylolysis, crossing laminar screw, lumbar laminar fixation, intralaminar screw, pedicle fixation alternative

INTRODUCTION

Lumbar spondylolysis (SL) refers to a defect in the pars interarticularis. The incidence of spondylolysis (SPL) in the general population ranges from 3% to 10% and is significantly influenced by ethnicity, sex, and physical activity levels[1-8]. Factors such as supraphysiological axial loading, chronic stress accumulation in the pars, repetitive hyperextension, rotation, flexion movements, and major trauma, alone or in combination, can cause SL[9-12]. SL most frequently occurs at the L5 level, followed by L4, with decreasing frequency at other lumbar levels[5,8,13,14]. Although typically asymptomatic, approximately 80% of symptomatic patients present with bilateral defects, whereas unilateral defects which follow a more benign course occur less frequently[15]. The primary complaint is localized lower back pain at the affected segment, which intensifies with activity and diminishes with rest. Pain may also radiate to the buttocks and posterior thigh and can be provoked by extension movements. Hamstring tightness is common and may contribute to postural abnormalities. Due to hamstring stiffness, flexibility may be reduced in straight leg raise tests[7,15,16]. Neurological examination findings are usually normal because isolated SPL does not cause nerve root compression. However, in cases of bilateral pars defects progressing to spondylolisthesis, L5 radicular pain, loss of reflexes, or rarely motor weakness may be observed[10,16-18].

The disease is typically diagnosed clinically and confirmed using imaging modalities, such as radiography, computed tomography (CT), magnetic resonance imaging (MRI), and single

Address for Correspondence: Burhan Oral Güdü, Sefaköy Medipol University Hospital, Department of Neurosurgery, İstanbul, Türkiye
E-mail: burhan.gudu@medipol.edu.tr
ORCID ID: orcid.org/0000-0002-5011-815X

Received: 16.05.2025 **Accepted:** 19.06.2025 **Publication Date:** 08.07.2025
Cite this article as: Güdü BO, Karan B. Bilateral crossing laminar screw fixation in lumbar spondylolysis: CT-based anatomical parameters. J Turk Spinal Surg. 2025;36(3):103-109

photon emission CT[11,12,19]. MRI is particularly valuable for detecting bone edema and stress reactions in young patients at the pre-lysis stage, especially when fractures are not visible on CT[7,11,20,21]. In addition, MRI provides ancillary findings that can significantly aid in the diagnosing SL[11]. The goal of treatment is to achieve pars bone fusion without surgical intervention. Conservative management leads to bone fusion in approximately 90% of cases, although this rate decreases in terminal-stage defects[2,18,22,23]. Surgical options may be considered when symptomatic back pain persists despite multiple conservative treatments or when neurological deficits develop[2,18,23,24]. Although the optimal surgical procedure remains controversial, direct and indirect surgical methods involving screws, rods, hooks, wires, cables, or combinations thereof are available for pars defect fixation[22,25,26].

Intralaminar screw fixation is preferred particularly in young adults with healthy intervertebral discs and positive pars injections[5,22,27]. In 1970, Buck[28] first reported a clinical success rate of 90% in pars defect fusion using an iliac bone graft and intralaminar screws. Subsequent studies have reported significant clinical success in pars defect repair aimed at preserving vertebral segmental mobility using laminar screws with both open and percutaneous surgical approaches[2,22,27]. Intralaminar screw fixation, a low-profile technique, facilitates the restoration of posterior vertebral arch anatomical integrity while preserving the motion segment[14,22,27]. Despite advancements in minimally invasive and robotic surgical techniques, no study has evaluated the anatomical parameters of lumbar crossing laminar screws (CLS) fixation in patients with symptomatic SPL. Thus, the objective of our study was to define the optimal CLS fixation trajectory in individuals with bilateral SL using the Centricity radiological workstation software on CT scans and to comprehensively analyze the linear and angular anatomical parameters along this trajectory.

MATERIALS AND METHODS

The study was approved by the İstanbul Medipol University Non-interventional Clinical Research Ethics Committee (decision number: 688, date: 19.07.2024). Methodological amendments to the study were subsequently approved and documented by the İstanbul Medipol University Non-interventional Clinical Research Ethics Committee on May 14, 2025 (reference number: E-10840098-202.3.02-3028). The study was conducted in accordance with the principles of the Declaration of Helsinki.

Inclusion criteria were as follows: 1) age between 18 and 80 years; 2) bilateral SPL; and 3) spondylolisthesis of 3 mm or less. The exclusion criteria were as follows: 1) postoperative patients with disrupted normal anatomical structures in the region of interest; 2) unsatisfactory image quality or metal artifacts; 3) congenital vertebral arch anomalies; 4) pedicle and/or vertebral body fractures; 5) infections; and 6) bone tumors. A total of 110 bilateral pars defects were analyzed.

The ideal CLS trajectory parameters were assessed by two independent observers using lumbar CT images obtained through oblique multiplanar reconstruction and real-time 3D axis manipulation on a radiology workstation (Centricity Universal Viewer; GE Healthcare, Chicago, IL, USA) with a slice thickness/increment of 1/1 mm (Figure 1). Observer 1 (BOG) performed all measurements twice to evaluate the intra-observer reliability.

Crossing the Laminar Screw Trajectory

For bilateral CLS trajectories, the screw entry points were selected at the lower third (1/3) and upper third (1/3) of the spinolaminar junction to avoid screw interference. The ideal CLS trajectory was defined as starting from the spinolaminar junction on the opposite side of the targeted pars defect; traversing through the intralaminar area, pars defect, pars neck, and pedicle; and terminating at the lateral or superior cortex of the pedicle (Figures 2 and 3). Additionally, the CLS technique was applied to a synthetic lumbar spine model and validated using fluoroscopic images and high-resolution 3D modeling (Figures 4 and 5).

Measured Anatomical Parameters (Figures 2 and 3)

1. Trajectory length: Maximum screw trajectory length from the spinolaminar junction opposite the defect to the pedicle cortical boundary.
2. Laminar height: Minimum laminar height along the screw trajectory in the parasagittal plane.
3. Laminar width: Bicortical width of the narrowest laminar

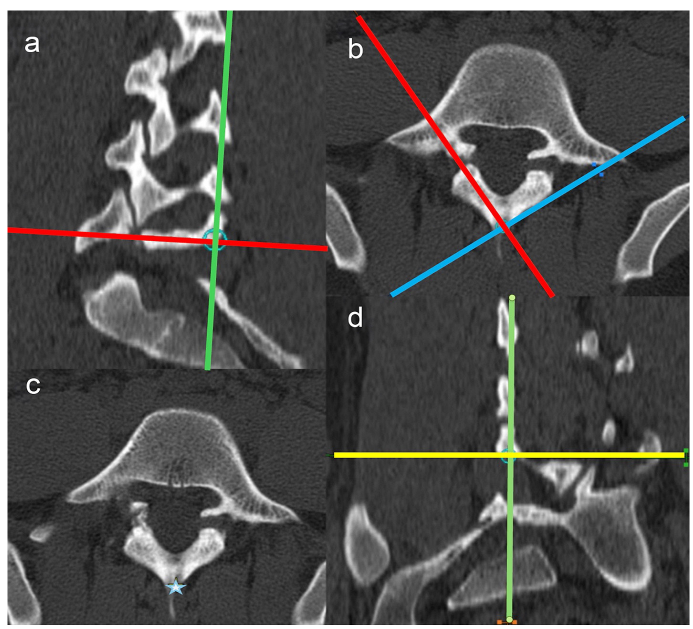

Figure 1. Three-dimensional computed tomography views in the parasagittal, axial, and coronal planes demonstrating the ideal trajectory for crossing laminar screw placement. (a) Parasagittal oblique reconstruction showing the full trajectory. (b) Axial view illustrating the screw path originating from the spinolaminar junction and passing through the laminar isthmus and pedicle. (c) Axial slice displaying the laminar entry zone. (d) Coronal plane showing the entry point of the screw

region in the axial plane.

4. Spinolaminar angle: Laminar angle of the screw trajectory from the spinolaminar entry point relative to the vertebral body.

5. Coronal angle: Angle of the screw trajectory in the coronal plane relative to the vertical axis.

6. Spinolaminar height: Maximum height measurement of the spinolaminar junction in the parasagittal plane.

Statistical Analysis

The normality of quantitative variables was assessed using the Shapiro-Wilk test and graphical methods (histogram, Q-Q plot, and box plot). The independent samples t-test was used to compare two groups of normally distributed variables, and the Mann-Whitney U test was used for non-normally distributed variables. One-way analysis of variance or Kruskal-Wallis tests were used to identify differences among the L3, L4, and L5 levels based on the variable distribution. Post-hoc analyses (Bonferroni or Dunn's tests) were performed to identify significant differences between the groups. Spearman's correlation analysis was conducted to examine the relationships between the vertebral levels and other quantitative variables, given the ordinal structure of the lumbar levels. Line graphs were created to visualize the trends.

Interobserver and intraobserver reliabilities were assessed using intraclass correlation coefficients (ICC). Interobserver reliability was assessed using a two-way random-effects model, absolute agreement, and single measures (ICC(2,1)). Intraobserver reliability was assessed using a two-way mixed-effects model, absolute agreement, and single measures (ICC(3,1)).

A distance error tolerance interval of ±0.5 mm (half of the maximum acceptable error level of 1 mm) was defined for each

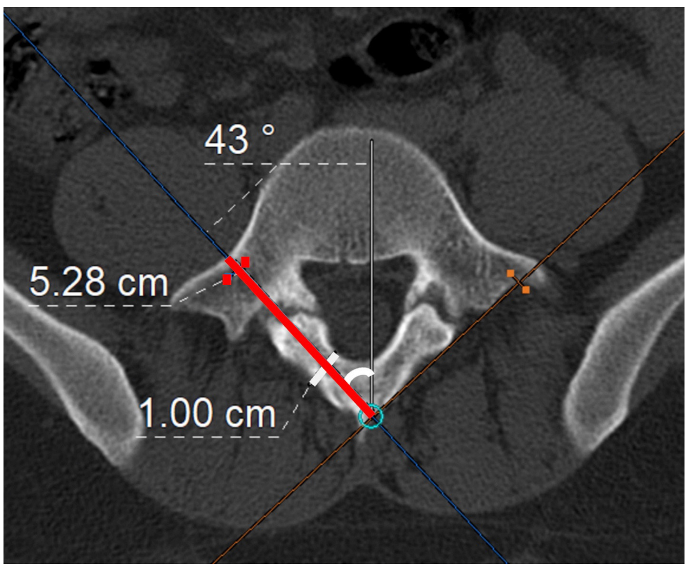

Figure 2. At the L5 level in the axial plane, the ideal trajectory length for crossing laminar screw placement was measured as 5.28 cm, with a spinolaminar angle of 43° and a laminar width of 1 cm

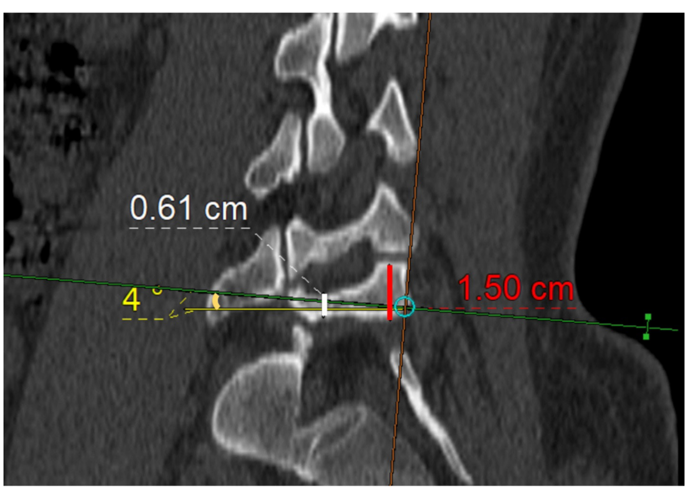

Figure 3. In the parasagittal oblique plane, the crossing laminar screw trajectory demonstrated an angle of 4° relative to the horizontal plane, a spinolaminar height of 1.5 cm, and a laminar height of 0.61 cm

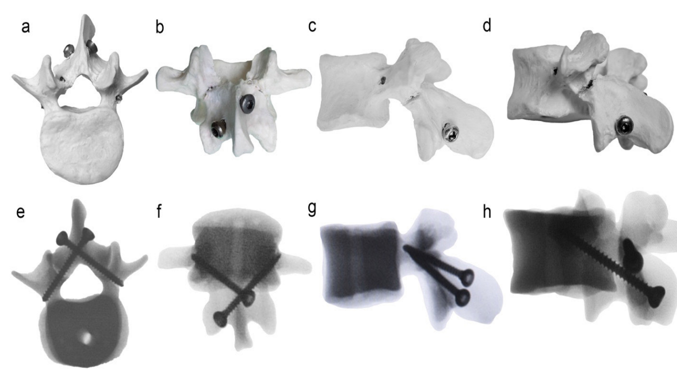

Figure 4. Multiplanar views of the L4 vertebral model with bilateral spondylolysis treated with crossing laminar screws. (a) Craniocaudal, (b) anteroposterior, (c) left lateral, and (d) left oblique views of the vertebra model. Corresponding intraoperative fluoroscopic images of the same vertebra are shown in the (e) craniocaudal, (f) anteroposterior, (g) left lateral, and (h) left oblique views

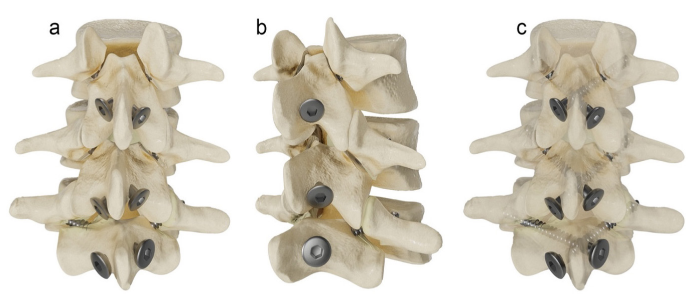

Figure 5. Three-dimensional high-resolution representations of bilateral crossing laminar screw fixation in L3-L4-L5 vertebral segments with spondylolysis. (a) Anteroposterior view, (b) right oblique view, (c) a detailed 3D model demonstrating the screw trajectories crossing through the lamina on both sides of the spinous process and terminating within the pedicles

measurement. This established an equivalence margin between -0.5 mm and +0.5 mm in the equivalence-based analytical design.

All statistical analyses were performed using SPSS Statistics for Windows (version 22.0; IBM Corp., Armonk, NY, USA). Statistical significance was set at p<0.05.

RESULTS

The age of the patients included in the study ranged from 18 to 80 years, with a mean age of 44±14 years. Lumbar CT revealed that SPL was most frequently observed at L5 (70%), followed by L4 (20%) and L3 (10%). The Centricity radiology workstation software facilitated the consistent identification of the ideal CLS trajectory line in all cases through real-time oblique multiplanar reconstruction. The screw trajectory originates from the spinolaminar junction; passes through the lamina slightly anteriorly, superiorly, and laterally; and terminates in the lateral or superior cortex of the pedicle. The morphology of the L5 lamina differs from that of L4 and L3, requiring more extensive axis manipulation at the L5 level. Significant differences were identified between L3, L4, and L5 for all linear and angular parameters (p<0.001) (Table 1).

Trajectory Length (mm)

The trajectory length was significantly longer at L5 (52±6 mm) compared to L4 (43±3 mm, p=0.002) and L3 (38±5 mm, p<0.001). The difference between L3 and L4 was not significant (p=0.756). These findings indicate a progressive increase in trajectory length from L3 to L5, with L5 demonstrating the longest trajectory.

Lamina Height (mm)

The highest lamina height was observed at L3 (11±3 mm), which was significantly greater than that at L4 (9±2 mm, p=0.002) and L5 (7±1 mm, p<0.001). The difference between L4 and L5 was not significant (p=0.148).

Lamina Width (mm)

The lamina width at L5 (10±2 mm) was significantly larger than that at L4 (7±1 mm; p=0.036) and marginally significantly larger compared to L3 (7±2 mm; p=0.087). There were no significant differences between the L3 and L4 groups (p=0.911).

Spinolaminar Angle (°)

The spinolaminar angle was significantly greater at L3 (45±2°) than that at L4 (40±4°, p=0.001) and L5 (40±3°, p=0.014). The difference between L4 and L5 was not significant (p=0.661).

Coronal Angle (°)

The coronal angle was largest at L3 (23±4°), significantly higher than that at L4 (14±6°, p<0.001) and L5 (9±4°, p<0.001), with a borderline significant difference between L4 and L5 (p=0.055).

Spinolaminar Height (mm)

The spinolaminar height was greatest at L3 (19±3 mm), significantly higher than that at L4 (15±4 mm, p=0.001) and L5 (14±5 mm, p=0.007), with no significant difference observed between L4 and L5 (p=0.777).

No significant differences were found between sexes or between the right and left sides (p=0.84). Additionally, there was no significant difference in the mean age between the groups (p=0.06). The repeatability of anatomical measurements at the L3, L4, and L5 levels was high, with inter-and intraobserver correlation coefficients approaching perfection, particularly for trajectory length, lamina height, and coronal angle parameters (Table 2).

Table 1. Mean (standard deviation) of crossing laminar screw trajectory at the L3, L4, and L5 laminae

Parameters	L3	L4	L5
Trajectory length (mm)	38 (5)	43 (3)	52 (6)
Lamina height (mm)	11 (3)	9 (2)	7 (1)
Lamina width (mm)	7 (2)	7 (1)	10 (2)
Spinolaminar angle (°)	45 (2)	40 (4)	40 (3)
Coronal angle (°)	23 (4)	14 (6)	9 (4)
Spinolaminar height (mm)	19 (3)	15 (4)	14 (5)

Table 2. Intraclass correlation coefficients and 95% confidence intervals for inter- and intra-observer reliability of laminar morphometric and angular parameters at L3, L4, and L5 levels

Parameters	L3	L4	L5
Trajectory length (mm)	0.936 (0.910-0.991)*	0.875 (0.524-0.917)	0.957 (0.939-0.978)
Lamina height (mm)	0.951 (0.891-0.974)	0.920 (0.90-0.994)	0.965 (0.927-0.980)
Lamina width (mm)	0.934 (0.710-0.966)	0.941 (0.870-0.9700)	0.864 (0.703-0.963)
Spinolaminar angle (°)	0.854 (0.731-0.902)	0.962 (0.940-0.970)	0.865 (0.761-0.934)
Coronal angle (°)	0.961 (0.927-0.980)	0.917 (0.890-0.940)	0.971 (0.953-0.988)
Spinolaminar height (mm)	0.871 (0.502-0.925)	0.923 (0.821-0.961)	0.850 (0.717-0.920)

*Mean (inter-reader reliability-intra-reader reliability)

DISCUSSION

In active individuals with symptomatic SPL, rigid fixation of the pars defect to the pedicle using intralaminar screws is recommended among surgical treatment options[5,22,29,30]. The CLS technique is particularly notable due to its low-profile design, preservation of the anatomical integrity of the posterior neural arch, and restoration of the motion segment. Our CT-based results evaluated the anatomical suitability of the CLS technique at the L3-L5 vertebral levels and highlighted the level-specific angular and linear variations. These findings provide a foundation for considering CLS as a surgical alternative for pars fixation.

With advancements in minimally invasive techniques for treating symptomatic SPL, segmental motion-preserving laminar screw techniques have become more prevalent[2,14,26,27]. Percutaneous laminar instrumentation offers significant advantages, including reduced tissue trauma, shorter hospitalization, minimized postoperative morbidity, and accelerated functional recovery[8,14,22,24]. The intralaminar screw technique described by Buck, which involves placement along the long axis of the lamina on the defect side, has successful fusion rates ranging from 60% to 100% in the literature[2,6,28,31]. Recent rapid advancements in robotic surgical systems and spinal navigation technologies have significantly enhanced the safety and clinical applicability of percutaneous laminar screw placement[1,5,27]. Although primarily utilized at the cervical and thoracic vertebral levels, the CLS technique emerges as an alternative to pedicle screws due to its high safety profile and potential for effective fusion[32-34].

Centricity imaging software facilitated the determination of the ideal screw trajectory for CLS through three-dimensional multiplanar reconstruction. The optimal CLS trajectory originates at the lamina–spinous process junction, equally divides the lamina and pars defects, and terminates within the pedicle, ensuring an optimal intracortical width. This ideal trajectory minimizes the risk of cortical breach and neural injury. The significant increase in trajectory length from L3 to L5 supports the use of longer screws at the L5 level. Longer trajectories may positively influence surgical outcomes by enhancing screw stability and pullout resistance. An increased laminar height at L3 allows for greater coronal angulation, whereas a reduced laminar height at L5 necessitates more cautious surgical intervention to avoid neural injury.

The lamina width at the L5 level was greater and thus suitable for thicker screws. Increased spinolaminar height at L3 suggests easier placement of crossing screws, whereas reduced height at L5 indicates a need for greater precision in screw angulation. The spinolaminar angle was slightly higher at L3 (45.0±2.0°), and the angular similarity between L4 and L5 supports for a more standardized surgical approach. The highest coronal angle was observed at L3 (23.0±4.0°), moderate at L4 (14.0±6.0°), and lowest at L5 (9.0±4.0°), indicating a requirement for more horizontal screw placement at caudal levels and more oblique placement at cranial levels. This variability in the coronal angle is critical for planning screw entry points and trajectories. A decreased coronal angle may require a more medial orientation for screw placement. Additionally, the coronal angle is crucial in evaluating for the risk of nerve root and dural injuries. Evaluation of the lamina heights and widths indicated that screws with a diameter of 4.5 mm could be safely placed without cortical violations across all assessed levels. CLS screws are typically 0.5-1 cm longer than those used in the traditional Buck technique, enhancing bone contact and thus improving screw stability[8,14,24].

In a study involving 173 patients who underwent translaminar facet screw fixation, a successful solid bone fusion rate of 94%, a screw loosening rate of 3%, and two cases of screw fracture were reported[35]. In terms of surgical technique, laminar screw fixation requires a similar level of surgical skill to pedicle screw fixation. This study provides anatomical data for CLS in the lumbar region and demonstrates its feasibility as an alternative to conventional methods. Successful bone fusion using bilateral percutaneous CLS placement with a robotic surgical technique was reported in a 16-year-old patient with SL[30]. Although the CLS technique is surgically feasible and relatively straightforward, mechanical stress and strain on the intralaminar screws may increase due to anatomical constraints in screw placement. Therefore, screws with the largest possible diameter and appropriate length should be used during laminar screw fixation[8,14]. Accurate anatomical parameters and angulation are critically important for laminar screw placement because penetration of the ventral surface of the lamina may result in spinal canal injuries. While no definitive minimum laminar thickness exists, the literature indicates that a minimum laminar thickness of 5 mm is adequate for screws with a diameter of 3.5 mm, noting that the lamina may be slightly expandable[33,36-38]. Screw diameter selection should be based on the lamina width, and alternative techniques should be considered accordingly.

A CLS trajectory should be applied parallel to the dorsal and superior edges of the lamina to prevent damage to the spinal canal. CLS is a technique that requires experience, and ensuring that screws remain intraosseous significantly reduces the risk of neural and dural injuries. However, variations in anatomical laminar thicknesses can complicate intraosseous screw placement, necessitating preoperative CT. Preoperative CT evaluation is critical to determine screw suitability, accurately identify entry points, and minimize potential complications[5]. Laminar screw fixation is described in the literature as a robust stabilization method with high fusion rates[2,22,27]. Although various techniques have been developed for the surgical repair of SPL, the thin laminar structure can decrease tensile strength, potentially leading to complications such as screw loosening, breakage, or pullout.

In anteroposterior and lateral radiographic views, the CLS hardware may appear asymmetric and unconventional. However, as with many spinal surgeries, surgeons must plan a technique that is best suited to the patient's anatomical structure. In other words, the advantages provided by the available bone structures should be optimally utilized for fixation, even if this does not always result in a symmetrical or aesthetically ideal appearance. In patients with posterior vertebral arch anomalies (e.g., hypoplastic or fractured lamina in high-grade spondylolisthesis, or absence of lamina, as observed in spina bifida), the CLS technique can be challenging or impractical.

Study Limitations

This study has several limitations. First, its retrospective and single-center design restricts the generalizability of the findings, highlighting the need for prospective, multicenter studies to enhance external validity. Second, the absence of cadaveric analyses and investigations into ethnic anatomical differences limits the broader applicability of the results across diverse populations. Third, the relatively small sample size further constrains the statistical power and generalizability of the findings, emphasizing the necessity for validation in larger cohorts. Finally, although the anatomical and radiological assessments provided detailed insights into the three-dimensional structure of the vertebral arch, these evaluations were not directly correlated with intraoperative observations, thus limiting their direct clinical relevance and translational applicability.

CONCLUSION

Analyses conducted at the L3, L4, and L5 vertebral levels in patients with SPL indicated that CLS screws with a diameter of 4.5 mm and a length of 4-5 cm could be safely placed using an oblique angle of approximately 10° at the L5 level and approximately 25° at the L3 level, combined with a lateral angulation of 40-45°. Utilizing advanced imaging methods in the preoperative period is crucial for determining the optimal screw trajectories, thereby ensuring stable and reliable bone fixation. Therefore, meticulous anatomical and radiological assessments during surgical planning can significantly enhance clinical outcomes.

Ethics

Ethics Committee Approval: The study was approved by the İstanbul Medipol University Non-interventional Clinical Research Ethics Committee (decision number: 688, date: 19.07.2024). Methodological amendments to the study were subsequently approved and documented by the İstanbul Medipol University Non-interventional Clinical Research Ethics Committee on May 14, 2025 (reference number: E-10840098-202.3.02-3028).

Informed Consent: Retrospective study.

Footnotes

Authorship Contributions

Surgical and Medical Practices: B.O.G., B.K., Concept: B.O.G., B.K., Design: B.O.G., B.K., Data Collection or Processing: B.O.G., B.K., Analysis or Interpretation: B.O.G., B.K., Literature Search: B.O.G., B.K., Writing: B.O.G., B.K.

Conflict of Interest: No conflict of interest was declared by the authors.

Financial Disclosure: The authors declared that this study received no financial support.

REFERENCES

1. Yurac R, Bravo JT, Silva Á, Marré B. Spondylolysis repair using a minimally invasive modified buck technique with neuronavigation and neuromonitoring in high school and professional athletes: technical notes, case series, and literature review. World Neurosurg. 2021;155:54-63.
2. Güdü BO, Aydın AL, Dilbaz S, Çiftçi E, Başkan F, Özer AF. Clinical results of restoration of pars ınterarticularis defect in adults with percutaneous ıntralaminar screw fixation. World Neurosurg. 2022;164:e290-9.
3. Logroscino G, Mazza O, Aulisa G, Pitta L, Pola E, Aulisa L. Spondylolysis and spondylolisthesis in the pediatric and adolescent population. Childs Nerv Syst. 2001;17:644-55.
4. Cho E, Kim GJ, Lee JE, Park HJ, Kim HJ. Eight-year prevalence trends of lumbar spondylolysis and isthmic spondylolisthesis in adolescent males: a population-based study from a nationwide military draft medical examination database in South Korea. World Neurosurg. 2024;190:e341-7.
5. Stewart JJ, Zhao DY, Pivazyan G, Gensler R, Voyadzis JM. Minimally invasive robot-assisted direct pars repair: illustrative cases. J Neurosurg Case Lessons. 2024;8:CASE2415.
6. Patel RD, Rosas HG, Steinmetz MP, Anderson PA. Repair of pars interarticularis defect utilizing a pedicle and laminar screw construct: a new technique based on anatomical and biomechanical analysis. J Neurosurg Spine. 2012;17:61-8.
7. Leone A, Cianfoni A, Cerase A, Magarelli N, Bonomo L. Lumbar spondylolysis: a review. Skeletal Radiol. 2011;40:683-700.
8. Güdü BO, Aydın AL, Mercan NE, et al. Anatomical parameters of percutaneous, minimally invasive, direct intralaminar pars screw fixation of spondylolysis. World Neurosurg. 2024;188:e567-72.
9. Vaccaro AR 4th, Divi SN, Kepler CK, Schroeder GD, Hecht AC, Dossett AB, et al. The management of acute lumbar stress reactions of the pedicle and pars in professional athletes playing collision sports. Clin Spine Surg. 2021;34:247-59.
10. Kobayashi A, Kobayashi T, Kato K, Higuchi H, Takagishi K. Diagnosis of radiographically occult lumbar spondylolysis in young athletes by magnetic resonance imaging. Am J Sports Med. 2013;41:169-76.
11. Karan B, Güdü BO. Lumbar spondylolysis: are ancillary magnetic resonance imaging findings useful in diagnosis? J Turk Spinal Surg. 2025;36:56-62.
12. Güdü BO, Karan B, Dilbaz S. Diagnostic efficacy of posterior epidural fat ınterposition on magnetic resonance t1-weighted sequence in the diagnosis of spondylolysis. World Neurosurg. 2024;191:e381-6.
13. Lin T, Zhang Z, Jiang Q, Yin J, Ma X, Wang C, et al. The joe-lin operative classification system for pediatric lumbosacral spondylolysis and spondylolisthesis. World Neurosurg. 2020;142:e18-31.
14. Menga EN, Jain A, Kebaish KM, Zimmerman SL, Sponseller PD. Anatomic parameters: direct intralaminar screw repair of spondylolysis. Spine (Phila Pa 1976). 2014;39:E153-8.

15. Debnath UK. Lumbar spondylolysis - current concepts review. J Clin Orthop Trauma. 2021;21:101535.
16. Berger RG, Doyle SM. Spondylolysis 2019 update. Curr Opin Pediatr. 2019;31:61-8.
17. Alqarni AM, Schneiders AG, Cook CE, Hendrick PA. Clinical tests to diagnose lumbar spondylolysis and spondylolisthesis: a systematic review. Phys Ther Sport. 2015;16:268-75.
18. Aoki Y, Kubota G, Inoue M, Takahashi H, Watanabe A, Nakajima T, et al. Age-specific characteristics of lumbopelvic alignment in patients with spondylolysis: how bilateral L5 spondylolysis ınfluences lumbopelvic alignment during the aging process. World Neurosurg. 2021;147:e524-32.
19. Ledonio CG, Burton DC, Crawford CH, Bess RS, Buchowski JM, Hu SS, et al. Current evidence regarding diagnostic imaging methods for pediatric lumbar spondylolysis: a report from the scoliosis research society evidence-based medicine committee. Spine Deform. 2017;5:97-101.
20. Cavalier R, Herman MJ, Cheung EV, Pizzutillo PD. Spondylolysis and spondylolisthesis in children and adolescents: I. Diagnosis, natural history, and nonsurgical management. J Am Acad Orthop Surg. 2006;14:417-24.
21. Ulmer JL, Mathews VP, Elster AD, Mark LP, Daniels DL, Mueller W. MR imaging of lumbar spondylolysis: the importance of ancillary observations. AJR Am J Roentgenol. 1997;169:233-9.
22. Menga EN, Kebaish KM, Jain A, Carrino JA, Sponseller PD. Clinical results and functional outcomes after direct intralaminar screw repair of spondylolysis. Spine (Phila Pa 1976). 2014;39:104-10.
23. Sairyo K, Katoh S, Sasa T, Yasui N, Goel VK, Vadapalli S, et al. Athletes with unilateral spondylolysis are at risk of stress fracture at the contralateral pedicle and pars interarticularis: a clinical and biomechanical study. Am J Sports Med. 2005;33:583-90.
24. Güdü BO. Comparison of clinical outcomes of conservative treatment, percutaneous intralaminar stabilization of pars defect, and posterolateral fusion with ınterbody fusion in spondylolysis. Med Records. 2025;7:94-9.
25. Gagnet P, Kern K, Andrews K, Elgafy H, Ebraheim N. Spondylolysis and spondylolisthesis: a review of the literature. J Orthop. 2018;15:404-7.
26. Yang X, Lin S, Chen HL, Liang J, Chen QQ, Xiao J, et al. Treatment of lumbar spondylolysis in young adults using modified intravertebral screw-rod fixation system for single vertebral body combined with autologous cancellous bone graft: a technical note and preliminary report. J Orthop Surg Res. 2024;19:868.
27. Narendran N, Nilssen PK, Walker CT, Skaggs DL. New technique and case report: robot-assisted intralaminar screw fixation of spondylolysis in an adolescent. N Am Spine Soc J. 2023;16:100284.
28. Buck JE. Direct repair of the defect in spondylolisthesis. Preliminary report. J Bone Joint Surg Br. 1970;52:432-7.
29. Ebraheim NA, Lu J, Hao Y, Biyani A, Yeasting RA. Anatomic considerations of the lumbar isthmus. Spine (Phila Pa 1976). 1997;22:941-5.
30. Yamashita D, Yamashita K, Sugiura K, Morimoto M, Manabe H, Tezuka F, et al. Robotic-assisted minimally invasive repair surgery for progressive spondylolysis in a young athlete: a technical note. J Surg Case Rep. 2024;2024:rjae085.
31. Lenke LG, Bridwell KH, Bullis D, Betz RR, Baldus C, Schoenecker PL. Results of in situ fusion for isthmic spondylolisthesis. J Spinal Disord. 1992;5:433-42.
32. Ilgenfritz RM, Gandhi AA, Fredericks DC, Grosland NM, Smucker JD. Considerations for the use of C7 crossing laminar screws in subaxial and cervicothoracic instrumentation. Spine (Phila Pa 1976). 2013;38:E199-204.
33. Wang MY. C2 crossing laminar screws: cadaveric morphometric analysis. Neurosurgery. 2006;59(Suppl 1):ONS84-8; discussion ONS84-8.
34. Jea A, Sheth RN, Vanni S, Green BA, Levi AD. Modification of Wright's technique for placement of bilateral crossing C2 translaminar screws: technical note. Spine J. 2008;8:656-60.
35. Humke T, Grob D, Dvorak J, Messikommer A. Translaminar screw fixation of the lumbar and lumbosacral spine. A 5-year follow-up. Spine (Phila Pa 1976). 1998;23:1180-4.
36. Dean CL, Lee MJ, Robbin M, Cassinelli EH. Correlation between computed tomography measurements and direct anatomic measurements of the axis for consideration of C2 laminar screw placement. Spine J. 2009;9:258-62.
37. Chytas D, Korres DS, Babis GC, Efstathopoulos NE, Papadopoulos EC, Markatos K, et al. Anatomical considerations of C2 lamina for the placement of translaminar screw: a review of the literature. Eur J Orthop Surg Traumatol. 2018;28:343-9.
38. Ma XY, Yin QS, Wu ZH, Xia H, Riew KD, Liu JF. C2 anatomy and dimensions relative to translaminar screw placement in an Asian population. Spine (Phila Pa 1976). 2010;35:704-8.